77-709

Aerodynamic Separation of Gases by Velocity Slip in Freejet Expansions

R. J. Cattolica* and R. J. Gallagher*
Sandia Laboratories, Livermore, Calif.
J. B. Anderson†
Pennsylvania State University, University Park, Pa.
and
L. Talbot‡
University of California, Berkeley, Calif.

An aerodynamic isotope separation technique based on the velocity slip between gases in a rarefied flow has been proposed. To evaluate this separation method, the velocity and translational temperature of the individual species in binary and ternary gas mixtures of argon and neon in helium have been studied in a low-density hypersonic freejet. The velocity and translational temperature of the gases were determined from the Doppler shift and broadening of the fluorescence excited by an electron beam. Monte Carlo simulation of the flowfield was also used to predict species velocity and temperature. Idealized separation factors α, calculated from both the experimental and theoretical results, exceeded the diffusive separation factor ($\alpha = 1.4$) for an argon-neon mixture. A maximum separation factor ($\alpha = 2.1$) was obtained from the measured gas properties.

Nomenclature

c = speed of light
C_6 = force constant for inverse sixth potential
D = orifice diameter
$G(v)$ = Maxwell-Boltzmann velocity distribution function
I = spectral line intensity
k = Boltzmann constant
Kn = Knudsen number
L = molar feed rate
$L(\nu)$ = natural line shape
m = mass
n = number density
P = pressure
r = radius
S = slip parameter
T = temperature
U = velocity
δw = separative work factor
x = distance along jet centerline
α = separation factor
β = angle with jet axis
γ = ratio of specific heats
κ = feedback constant
ν = frequency
θ = gas fraction in enriched stream
$\Upsilon(\nu)$ = interferometer transfer function
μ = reduced mass

Subscripts

$*$ = sonic conditions
0 = source conditions
$\parallel$ = parallel direction
$\perp$ = perpendicular direction
max = maximum value
min = minimum value
avg = average value

Introduction

THE need to find methods for separating isotopes, which are more energy efficient than the current diffusion process, has stimulated research in the development of a number of separation schemes.[1] Among the newest of these techniques[2] is one that makes use of the velocity slip that occurs in the rarefied expansion of a mixture of a heavy molecular weight gas and a lighter molecular weight carrier gas in a nozzle or freejet. If the heavy gas is an isotopic mixture, conditions of the expansion can be selected such that an appreciable differential velocity slip between the heavy isotopic species can be obtained.

Previous experimental work[3-6] with molecular beams has consisted of measuring terminal velocity slip and speed ratios in binary mixtures and correlating the results with a modified source Knudsen number. Extrapolating these results, theoretical separation factors two orders of magnitude larger than that obtained in gaseous diffusion have been predicted[2] for separating $^{235}UF_6$ and $^{238}UF_6$. To put such an ex-

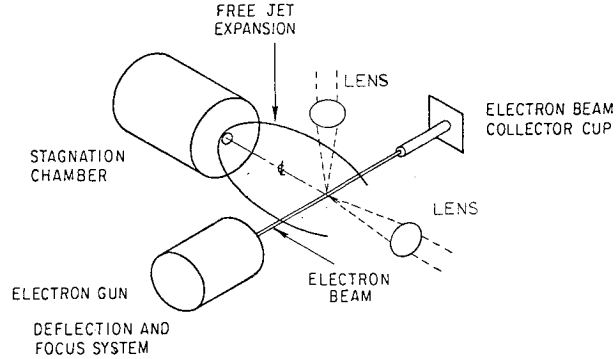

Fig. 1 Experimental appartus in low-density wind tunnel.

Presented as Paper 77-709 at the AIAA 10th Fluid & Plasmadynamics Conference, Albuquerque, N. Mex., June 27-29, 1977; submitted Dec. 12, 1977; revision received Nov. 17, 1978.

Index category: Rarefied Flows.
*Member of the Technical Staff. Member AIAA.
†Professor, Dept. of Chemistry.
‡Professor, Dept. of Mechanical Engineering. Member AIAA.

trapolation on a firmer basis, a more detailed understanding of the nonequilibrium phenomenon involved, particularly for ternary gas mixtures, is necessary for an accurate estimation of the separation effect.

In the work which is reported, individual species velocity and translational temperature have been studied in binary and ternary gas mixtures of argon and neon in helium in low-density freejet expansions. Velocity slip and translational nonequilibrium have been observed and the resultant separation efficiency for argon and neon has been calculated. In addition, a numerical simulation of the expansion of the gas mixtures using a Monte Carlo technique has also been developed and the results compared. Comparison with a modeled Boltzmann equation solution is also included.[7]

Experimental Technique

The experimental setup for this study is illustrated in Fig. 1. A freejet expansion through a thin plate orifice (6.35 mm diam) is produced from a stagnation chamber exhausting into a continuously pumped, low-density wind tunnel. The stagnation chamber is mounted on a traverse mechanism and can be positioned in space with an accuracy of ± 0.03 mm. Simple achromatic lenses (55 mm $f/5$) are mounted parallel and perpendicular to the freejet centerline and focused on an electron beam (approximately 1 mm diam) which was typically operated at 28 keV and 1-20 mA. Additional mirrors and a solenoid-operated shutter mirror, which could be controlled by a computer, allowed alternate observation of the electron beam-excited fluorescence parallel and perpendicular to the centerline of the freejet. The argon, neon, and helium mixtures studied were supplied premixed or mixed in a prechamber through sonic orifices with the pressure ratio in the stagnation chamber adjusted to give the proper composition.

The electron beam-excited fluorescence,[8] for the monatomic gases studied is composed of individual spectral lines which are Doppler shifted and broadened by their corresponding species velocity distribution function. The frequency shift of an electronic transition ν_0 excited in the fluorescence is related to the velocity u of the gas relative to an observer by the Doppler relation:

$$\frac{\Delta\nu}{\nu} = \frac{\nu - \nu_0}{\nu_0} = \frac{u}{c} \tag{1}$$

where c is the speed of light. For the gases used in this study, the following transition frequencies were observed: helium, 19937.52 cm^{-1}; neon, 17088.17 cm^{-1}; and argon, 21693.86 cm^{-1}.

To observe these individual spectral lines, a Fabry-Perot interferometer and grating monochromator were used (Fig. 2). The monochromator is used to isolate a particular spectral line, which could then be analyzed with the high resolution of the Fabry-Perot interferometer. Both are controlled by a computer, the interferometer is piezoelectrically scanned, and the monochromator is positioned by a micrometer driven by a stepping motor.

To measure the Doppler shift of an individual spectral line and thus the velocity of a particular species, the position of the line relative to a known reference must be determined. For this experiment, the radiation viewed perpendicular to both the centerline of the jet and the electron beam is used as the reference. Since there is no radial velocity component on the centerline of the axisymmetric jet, the Doppler shift between the spectral line observed perpendicular and parallel to the jet centerline will give the axial velocity of the gas along the central streamline. Since the flow is approximately source-like along the jet centerline, the assumption of a zero velocity shift for the perpendicular distribution function will break down as the measurement position is moved away from the centerline. The reference line is no longer at zero velocity, but is itself Doppler-shifted by a velocity component $U_\perp = \sin\beta \cdot U_\parallel$, where β is the angle of the measurement position with respect to the origin of the jet. The breakdown of this assumption is the principle error in the velocity measurement.

The position of the reference line and the Doppler-shifted line are determined from scanning the spectral lines with the Fabry-Perot interferometer. Instead of recording the entire spectral line, only selected points at the center, left, and right half-intensity positions are observed and used to determine the line position and width. After an initial approximation to these positions is obtained, a computer algorithm is used which tracks these positions using a linear feedback technique. In the Doppler shift measurement, the perpendicular and parallel spectral lines are alternately tracked by the computer. The line centers and widths are averaged over a number of cycles. The difference in the averaged line center positions gives the Doppler shift.

The accuracy of this velocity measurement technique was determined by studying equilibrium freejets (i.e., no velocity slip or translational nonequilibrium) over a range of argon and helium mixtures. Velocity measurements were taken on the jet centerline at $x/D = 12$. At this position, a ± 0.5-mm misalignment of the electron beam and optics normal to the jet centerline introduces a velocity error of less than $\pm 0.5\%$. The entrance aperture of the monochromator defined a 1-mm section through the electron beam at the measurement position. With an electron beam diameter of 1 mm (Gaussian

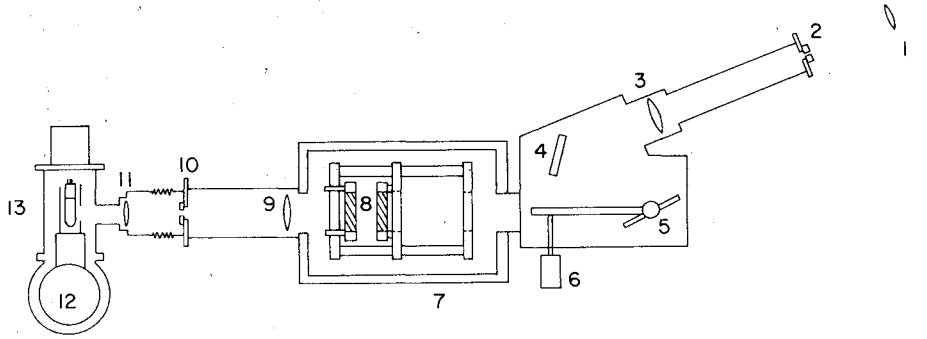

1 - Lens
2 - Rectangular aperture
3 - Lens
4 - Mirror
5 - Diffraction grating 600 lines per mm and 48° blaze angle
6 - Grating stepping motor
7 - Constant temperature, interferometer chamber
8 - Piezoelectrically scanned Fabry-Perot interferometer
9 - Lens
10 - Rectangular aperture
11 - Lens
12 - Liquid nitrogen reservoir
13 - Photomultiplier used in photon counting mode

Fig. 2 Fabry-Perot interferometer and grating monochromator.

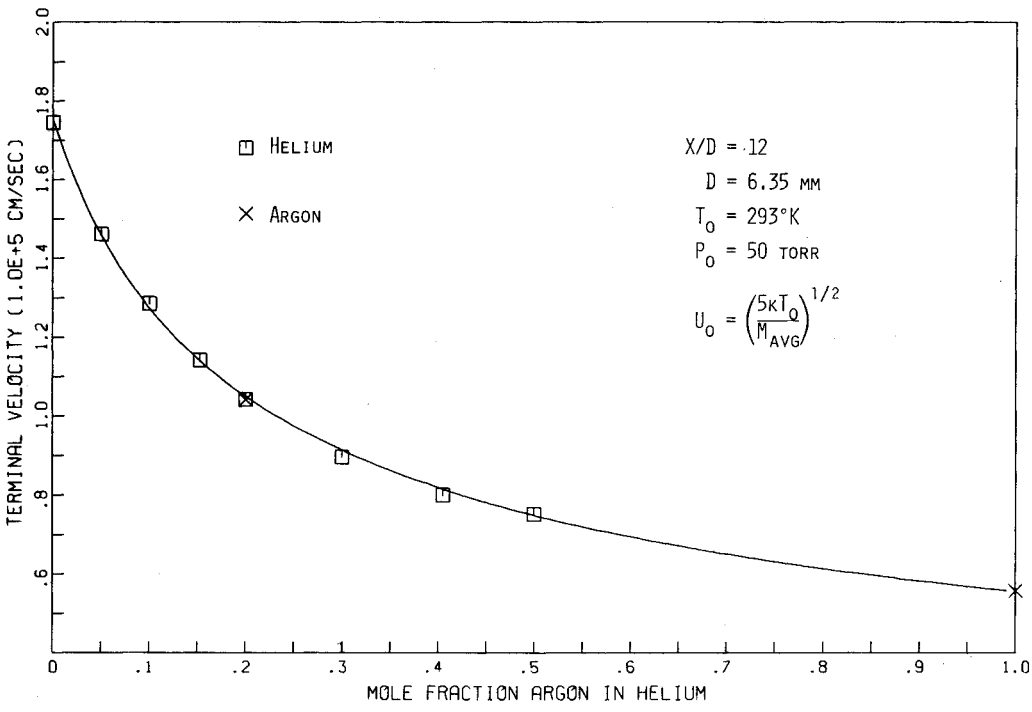

Fig. 3 Terminal velocity measurements for argon-helium mixtures.

half-width), any misalignment greater than ±0.5 mm could be observed and corrected.

For the velocity measurement, the interferometer plate spacing was 1.6 cm, giving a free spectral range of 0.31 cm^{-1}. With a fineness of 18.5, the resolution or bandwidth of the system was 0.016 cm^{-1}. To maximize the signal, this bandwidth was chosen to be comparable to the line width of the Doppler-broadened spectral lines. The data from these measurements are presented in Fig. 3. For convenience, most of the measurements were taken with helium because of its more intense fluorescence signal relative to argon, but a few argon measurements are also included. The calculated terminal velocities, U_0 are obtained from the energy equation for a gas mixture expanded to zero pressure or temperature.

$$U_0 = \left(\frac{2\gamma}{\gamma - 1}\frac{kT_0}{m_{\text{avg}}}\right)^{1/2} \tag{2}$$

where T_0 is the stagnation temperature, m_{avg} is the average molecular mass of the mixtue, and γ is the ratio of specific heats. The agreement between the measured and calculated terminal velocities is within the expected experimental accuracy of ±0.5%.

The measurement of gas temperature from the width of a spectral line is complicated by additional broadening effects introduced by the natural linewidth of the electronic transition which is observed and the finite bandwidth of the Fabry-Perot interferometer. Both of these additional broadening effects are independent of the gas temperature. The spectral profile from the interferometer $S(\nu)$ can be modeled by the following convolution:

$$S(\nu) = \iint G(\nu - \nu', T) L(\nu' - \nu'') \Upsilon(\nu'') \, d\nu' \, d\nu'' \tag{3}$$

where $G(\nu, T)$ is a Maxwell-Boltzmann velocity distribution function at a temperature T transformed to frequency space with the Doppler relation, $L(\nu)$ is the natural line shape of the electronic transition, and $\Upsilon(\nu)$ is the transfer function of the Fabry-Perot interferometer. The natural line shape is a Lorentz function whose half-width is determined from the lifetime of the transition. The transfer function can be approximated analytical[9] as an Airy function, which has a dependence on the interferometer plate reflectivity, roughness, and parallelism; convoluted with an aperture function for the system.

A preferable technique for determining the transfer function for the Fabry-Perot interferometer is the direct measurement of the spectral profile of a source much narrower than the transfer function. For the helium transition at $\nu_0 = 19937.52$ cm^{-1} (5015.67 Å), a near coincidence occurs with the 5017 Å line from an argon-ion laser. This line is sufficiently narrow, with the laser operated in a single longitudinal mode, so that it can be used in the manner of a Dirac delta function to measure the transfer function of the interferometer.

Using the transfer function $\Upsilon(\nu)$ measured with the argon laser and a Lorentz function for the natural line shape $L(\nu)$ for the helium $3\,{}^1P - 2\,{}^1S$ transition with a half-width of $\Delta\nu_L = 0.003$ cm^{-1}, the convolution defined by Eq. (4) was integrated numerically for specific temperatures. From the calculated spectral profile, the linewidth at the half-peak intensity position could be determined as a function of temperature. Because the transfer function of the Fabry-Perot interferometer is a periodic function, successive orders overlap and a minimum intensity I_{min} exists between them. A second modified linewidth at the $(I_{\text{max}} + I_{\text{min}})/2$ position of the spectral line was also determined as a function of temperature from the calculated spectra. This latter linewidth has the advantage of being independent of any baseline which would add to the spectral profile. Although the photon-counting detection system used in the signal acquisition had a dark rate less than 1 count/s, at the lowest signal levels to be measured (~50 counts/s), scattered light in the optical system could introduce a significant baseline.

The measurement of the helium gas temperature using this modified linewidth was evaluated in an equilibrium jet of pure helium. The results of a flowfield survey along the jet centerline are plotted in Fig. 4. Since the flowfield is source-like along the axis of the jet, the temperature distribution can be modeled by a one-dimensional expansion from a sphere of sonic radius r_*. Using the hypersonic assumption that $U \simeq U_0$, the temperature distribution can be determined explicitly from the continuity equation as:

$$\frac{T}{T_0} = \left(\frac{2}{\gamma + 1}\right)\left(\frac{\gamma - 1}{\gamma + 1}\right)^{(\gamma - 1/2)} (x/r_*)^{-2(\gamma - 1)} \tag{4a}$$

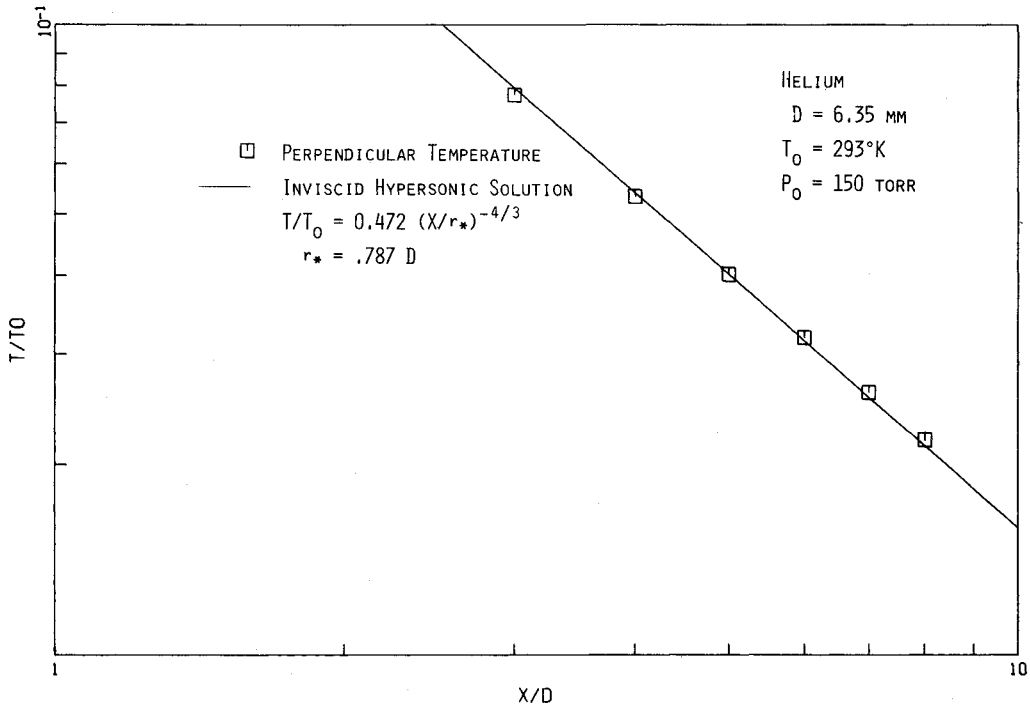

Fig. 4 Temperature distribution along the centerline of an inviscid freejet.

or with $\gamma = 5/3$ for helium

$$T/T_0 = 0.472(x/r_*)^{-4/3} \tag{4b}$$

The agreement between the measured and calculated temperature distribution is excellent with the error being less than 1%. The value of $r_* = 0.787\ D$ was obtained by a best fit of the temperature power law dependence. This value for r_* is consistent with previous analytical[10] and experimental[11] determinations.

Since there were no coincidences between the argon-ion laser lines and the argon and neon lines that were used in the electron beam-excited fluorescence, the transfer function at these wavelengths could not be measured directly. Instead of attempting an analytical modeling of the transfer function, a direct calibration of the linewidth vs temperature relationship for neon and argon was made. This calibration was obtained by making flowfield surveys along the axis of equilibrium jets with binary mixtures of argon in helium and neon in helium. The temperature of the argon or neon was determined from the helium linewidth measurement.

Monte Carlo Simulation

Under the conditions required for operation of the velocity slip process, a gas mixture passing through a slit or orifice moves from a region of continuum flow near the nozzle exit into a transition region and finally into free-molecular flow at a distance downstream. The expansion process is not amenable to treatment by the techniques of either continuum or free molecular gasdynamics. Although a kinetic model for the Boltzmann equation developed by Brook and Oman,[12] Hamel and Willis,[13] and Cooper and Bienkowski[14] has been successfully applied by Anderson[15] in predicting velocity distributions for helium-argon mixtures, the method of choice is the direct-simulation Monte Carlo method originated by Bird[16] in which molecules are followed individually in motion through the flowfield and in collisions with each other. The method has been applied previously to single-component freejet expansions and has faithfully reproduced experimentally observed velocity distributions.[17] It has also been applied in calculations to predict the extent of separation by velocity slip for $He/UF_6/UF_6$ mixtures.[18]

For the experiments reported, a corresponding Monte Carlo calculation has been performed to predict species temperatures and velocities. As in previous studies,[17,18] the axisymmetric freejet was treated as a source flow in which expansion occurs in a radial direction from a spherical entry surface of radius r_0. The soucelike behavior of the jet along its centerline has been documented by method-of-characteristics calculations of the streamlines[10] and by experimental measurements[11] of the density ($\rho \sim r^{-2}$) and temperature ($T \sim r^{-4/3}$) dependence for monatomic gases. The upstream boundary for the simulation was specified as the sonic radius, $r_0 = r_*$, with flow conditions corresponding to equilibrium at Mach number $M = 1$.

The calculations were carried out using a modification of the computation methods employed by Bird[16] for selecting collision partners. Collisions were treated as for hard spheres, but collision cross sections were adjusted according to the omega integrals[19] for a Lennard-Jones 6-12 potential between partners. For a given relative velocity between species, the temperature required for a mean relative velocity equal to that velocity was computed; the cross section $\pi\Omega^2$ was adjusted by the factor $\Omega^{(1,1)}$ for that temperature and the Lennard-Jones parameters for the interaction. The Lennard-Jones parameters used were: He-He, $\epsilon/k = 10.8$, $\sigma = 2.57$; He-Ne, $\epsilon/k = 22.9$, $\sigma = 2.685$; He-Ar, $\epsilon/k = 65.4$, $\sigma = 2.99$; Ne-Ne, $\epsilon/k = 35.0$, $\sigma = 2.8$; Ne-Ar, $\epsilon/k = 77.5$, $\sigma = 3.105$; Ar-Ar, $\epsilon/k = 120$, $\sigma = 3.41$ (in K and Å).

The computation was divided into two parts: one for $1 < r/r_0 < 11$, the other for $11 < r/r_0 < 110$. Step size in distance was $0.1\ r_0$ for the inner section and $1.0\ r_0$ for the outer with $r_0 = 1$ cm. Time step was 5×10^{-7} s for the inner section and 5×10^{-6} for the outer. Properties of the molecules leaving the inner section were stored and used subsequently for computing the feed to the outer section. The number of molecules per cell was approximately 20. Velocity distributions of each species were determined from the accumulated data at selected points in the flowfield and included data from 13,000 molecules in a typical run. From these velocity distribution functions, species temperature, mean velocities, and most probable velocities were determined.

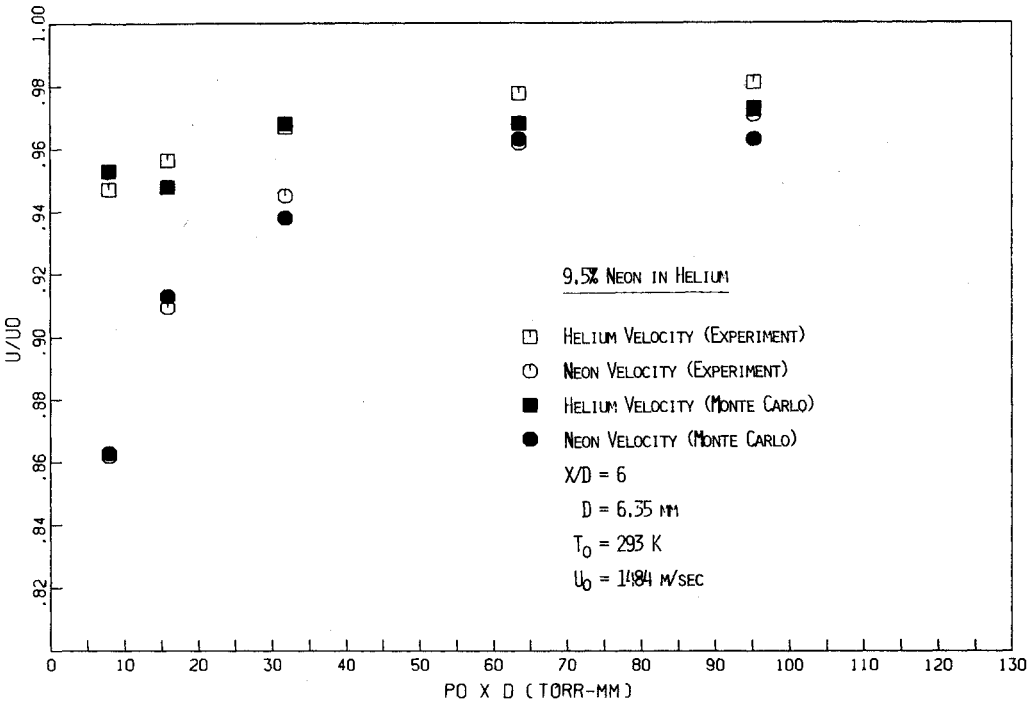

Fig. 5 Velocity as a function of source pressure for 9.5% neon in helium.

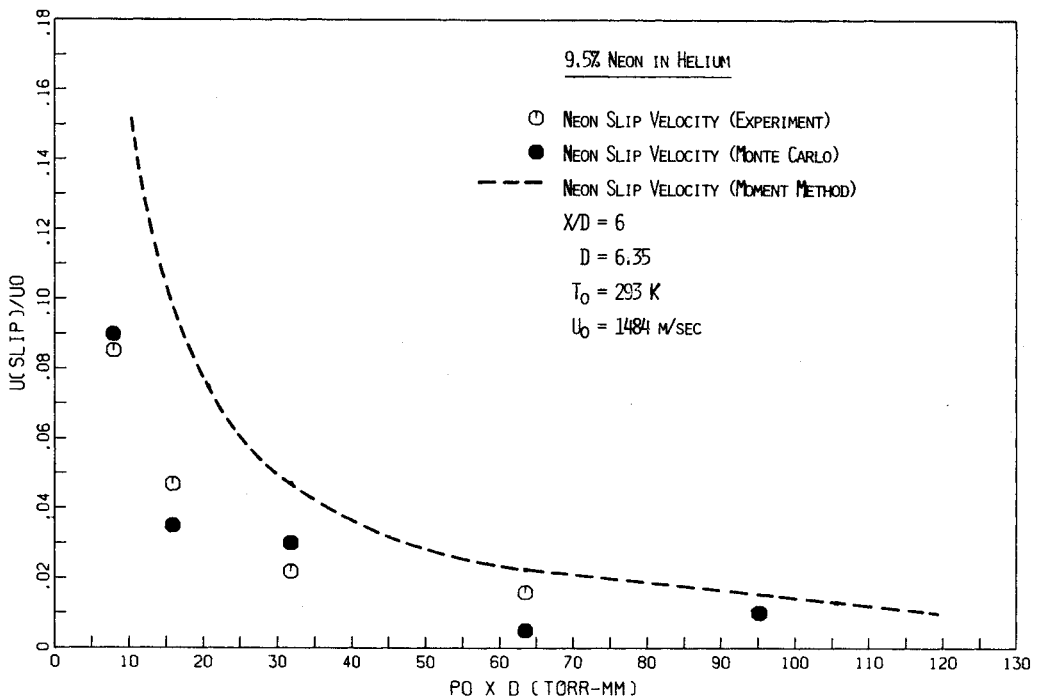

Fig. 6 Velocity slip as a function of source pressure for 9.5% neon in helium.

Results

Using the techniques described in the previous section, the velocity and temperature of individual species were studied in low-density freejet expansions of both binary and ternary mixtures of argon, neon, and helium. Gas mixtures of 9.5% Ne in He, 10.1% Ar in He, and 10.1% Ne, 9.8% Ar in He were used. These gases were provided premixed with the composition determined by mass spectroscopy. For the binary mixtures, the composition could also be determined by measurement of the terminal velocity.

All the data presented were obtained on the jet centerline at $x/D=6$; this was necessary to maintain sufficient signal intensity from the fluorescence (particularly for the low-level signals from argon and neon), so that the noise due to the Poisson statistics of the photon counting did not degrade the accuracy of the line-tracking algorithm. The velocity measurements for the binary and ternary gas mixtures as a function of source pressure are presented in Figs. 5-10. The velocity and velocity slip have been normalized by the terminal velocity U_0 defined by Eq. (2). The data have been plotted against $P_0 \times D$ which is proportional to the inverse source Knudsen number. The open symbols are the experimental measurement; the solid symbols are the comparable Monte Carlo result.

For the binary and ternary mixtures, the velocity slip between the various species is apparent as the source pressure is decreased. Even at the highest pressure, the measured velocities are less than the equilibrium value. At the position where the data were obtained, the static temperature is not negligible and the effect of translational nonequilibrium can

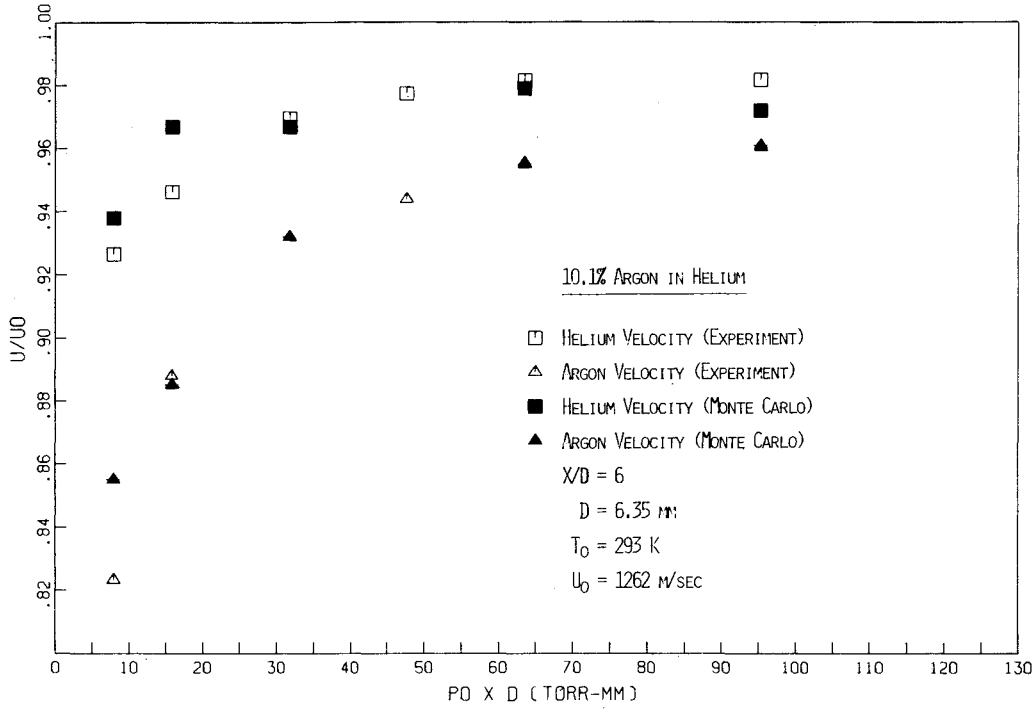

Fig. 7 Velocity as a function of source pressure for 10.1% argon in helium.

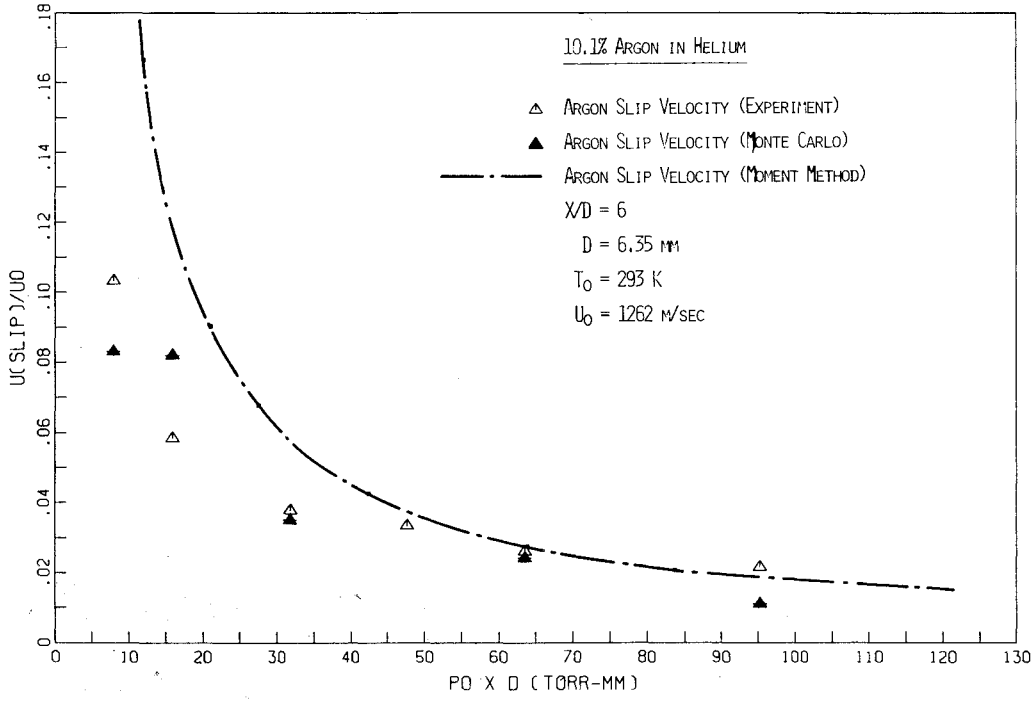

Fig. 8 Velocity slip as a function of source pressure for 10.1% argon in helium.

freeze substantial energy in the parallel distribution function, which otherwise would appear as directed kinetic energy. The decrease in the heavy minor species velocities results from a combination of the severe translational nonequilibrium and the velocity slip which occurs as the source pressure is lowered.

The agreement between the Monte Carlo simulation and the measured velocity for the heavy molecular species (argon and neon) is good, the error being about 1%. The agreement with the velocity of helium, which is the carrier gas, is not as close. The Monte Carlo simulations predict higher velocity (as much as 3%) with larger scatter. The predicted specie velocities were obtained from the most probable velocity, defined as the peak at the velocity distribution function. This is the velocity that corresponds to the experimental measurement which defines the velocity from the peak position of the spectral line. In the initial presentation of this work,[20] the velocity was defined by taking a moment of the distribution function. Higher velocities were predicted because of the effect of a non-Maxwellian population in the high-velocity tail of the distribution function. This phenomenon has been observed previously in both experimental measurements and discrete ordinate calculations.[21]

The moment method results for the velocity slip between the helium carrier gas and heavier molecular weight species are plotted in Figs. 6, 8, and 10. Since the moment equations are cast explicitly in terms of the velocity slip, the actual velocities are not available. For the binary gas mixtures, the predicted velocity slip agrees with the Monte Carlo and experimental results, except at the lowest values of P_0D. Under

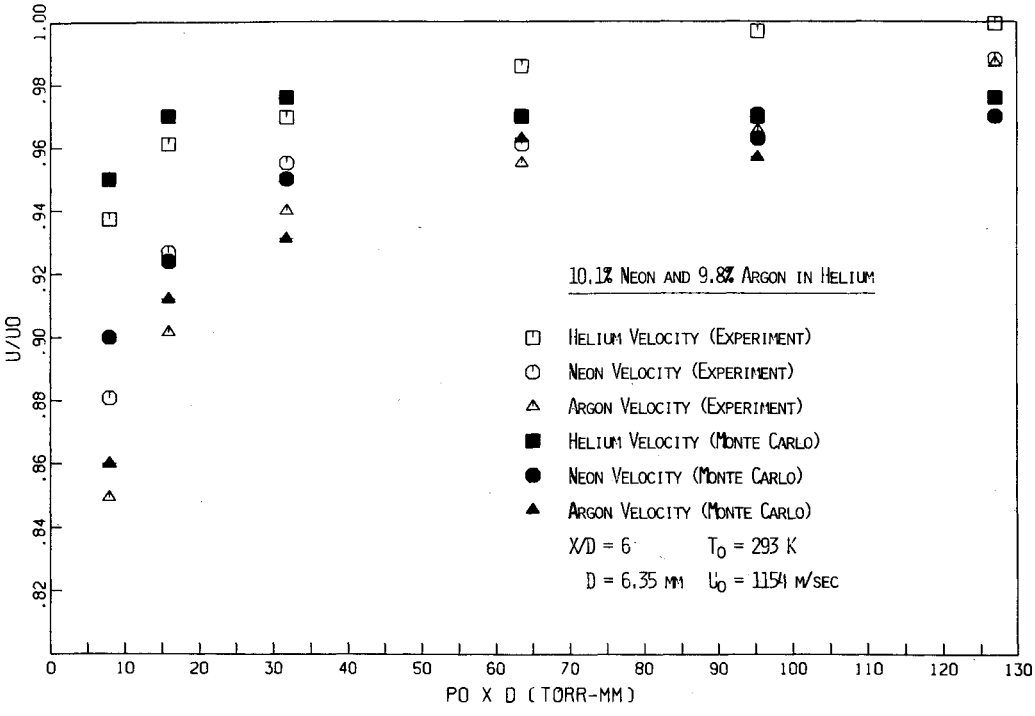

Fig. 9 Velocity as a function of source pressure for 10.1% neon and 9.8% argon in helium.

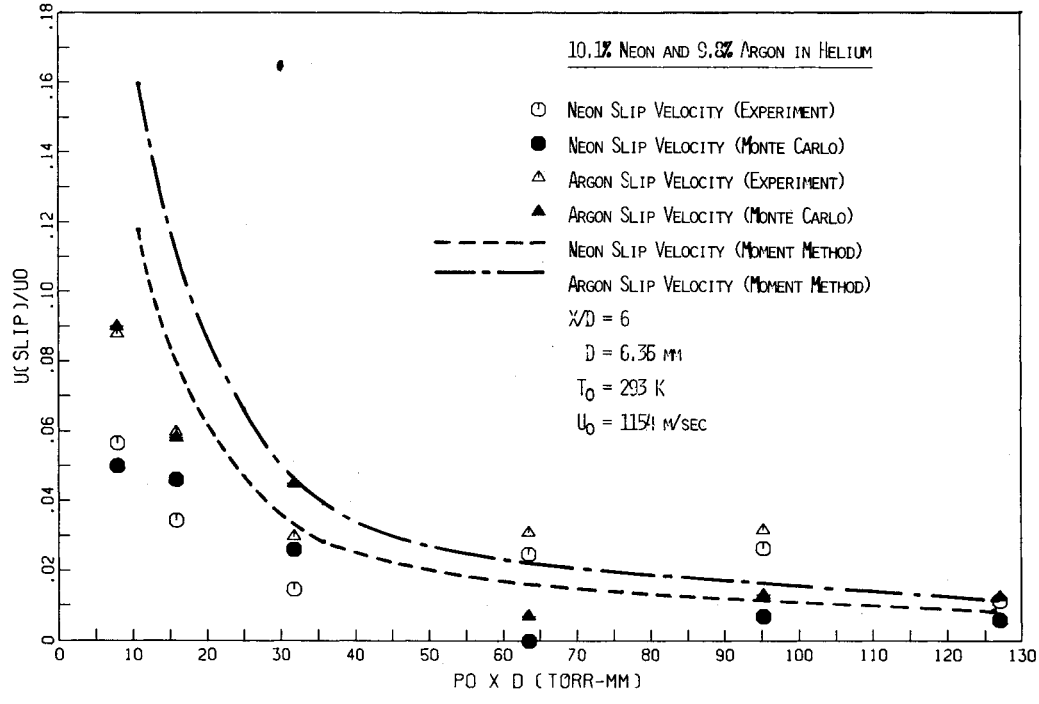

Fig. 10 Velocity slip as a function of source pressure for 10.1% neon and 9.8% argon in helium.

these conditions, the breakdown in the hypersonic approximation used to truncate the moment equations contributes significantly to this error. Since the calculated velocities from the moment solution are the result of moments of the appropriate distribution functions, they will reflect the non-Maxwellian effects encountered at the most rarefied conditions. The velocities from Monte Carlo simulation and the experimental data are the most probable velocities and correspond to the peak of the velocity distribution function. The moment solution for the ternary gas mixtues follows the same behavior, predicting larger velocity slip as the flow conditions become more rarefied. The differential slip (the difference between the argon and neon slip), which is the important parameter for a separation scheme, however, is in good agreement with both Monte Carlo and experimental results.

The velocity slip for all the mixtures can be correlated by plotting the normalized velocity slip U_{slip}/U_0 against a slip parameter S using Fig. 11. This slip parameter is a modified inverse source Knudsen number suggested by Miller and Andres[4]

$$S = \frac{(\mu_{12} M_{avg})^{1/2}}{|M_1 - M_2|} \frac{P_0 D}{(kT_0)^{4/3}} [6C_6(1,2)]^{1/3} \qquad (5)$$

where μ_{12} is the reduced mass, M_{avg} is the average mass, P_0 is the stagnation pressure, T_0 is the stagnation temperature, D is the orifice diameter, and C_6 is the constant for an inverse sixth potential between appropriate species.[22] For the ternary species, the inverse sixth potential for the helium interaction was used. The average mass of the mixture, however, was modified by the mole fraction of the second minor species

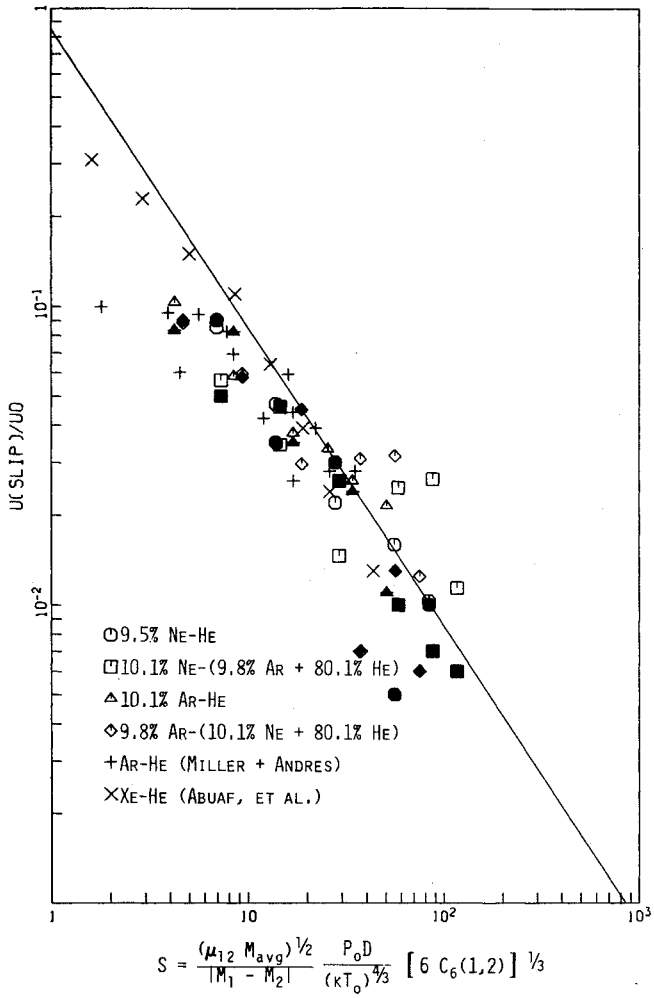

Fig. 11 Correlation of normalized velocity slip with slip parameter (solid symbols are Monte Carlo calculations).

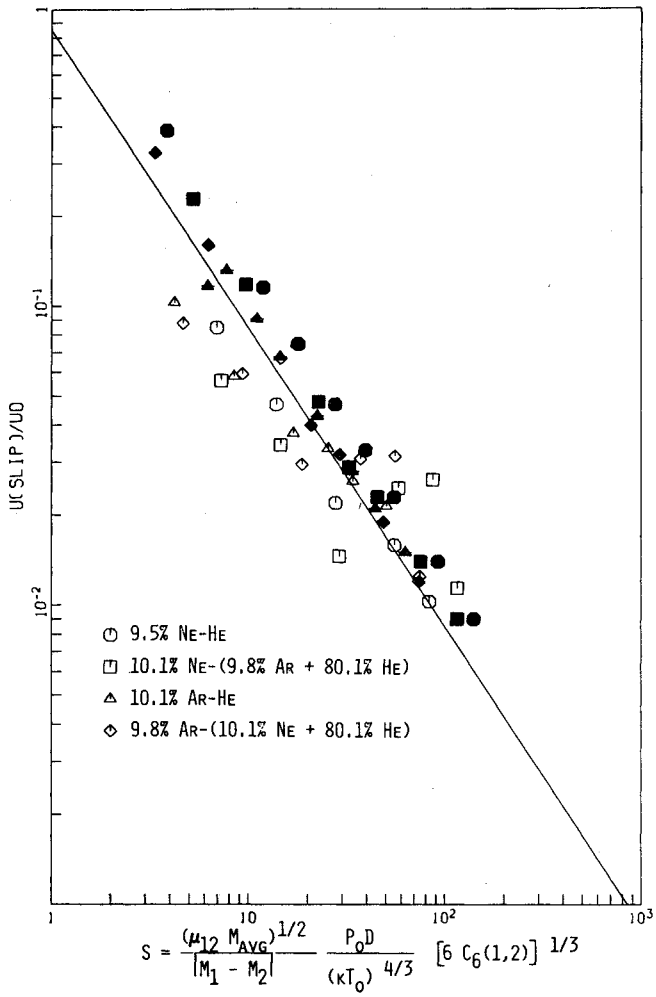

Fig. 12 Correlation of normalized velocity slip with slip parameter (solid symbols are moment method calculations).

present. Although there is considerable scatter in these data, the agreement between the electron beam fluorescence data and the molecular beam data is good. The ternary gas data are somewhat difficult to interpret with a slip parameter which is defined for a binary gas. The solid line represents the theoretical results of Miller and Andres, which predicts a S^{-1} dependence for U_{slip}/U_0. The qualitative agreement with all the data is reasonable and show the general trend in the behavior of the velocity slip with the slip parameter. The scatter in the Monte Carlo simulation results is similar to that from the experiments. Data below 1-2% slip should not be considered seriously since that approaches the accuracy of the measurements.

The velocity slip results from the moment method calculations are plotted (solid symbols) against the correlating slip parameter S in Fig. 12. The agreement with the experimental data is good, with the scatter being similar, but predicting larger slip, particularly for the most rarefied conditions. The scatter in the moment results is such that the $S^{-12/11}$ dependence for U_{slip}/U_0, developed in the moment method solution,[7] is not easily differentiated from the S^{-1} dependence predicted by Miller and Andres.

Since the velocity slip occurs along a streamline, the temperature which is important for a separation process is the parallel temperature. Using a modified linewidth based on the $(I_{max} + I_{min})/2$ positions, the parallel temperatures for the binary and ternary mixtures were measured at the same axial positions and source conditions as the previous velocity measurements. The helium temperature was determined from linewidth calculations. The argon and neon temperatures were based on the linewidth calibration measurements which were described previously.

The increase in parallel temperature with decreasing pressure follows the expected trend as the translational nonequilibrium effects move further upstream. The measured helium temperature is higher than the argon temperature throughout the range of source pressure which was studied. The predicted helium temperatures from the Monte Carlo and moment method calculations are in reasonable agreement with the experiment. The larger departure being at the lowest source pressure where the assumptions used in the two techniques becomes tenuous. The non-Maxwellian behavior of the velocity distribution function and the breakdown of the hypersonic approximation for the moment solution become serious errors at these most rarefied conditions. For the Monte Carlo solution, the equilibrium boundary conditions at the sonic surface where the flow simulation is initiated begin to break down.

The argon parallel temperature being lower than the helium temperature throughout the range of source pressures studied disagrees with both the Monte Carlo and moment solution results. This translational nonequilibrium or freezing of the parallel temperatures is illustrated by the Monte Carlo simulation of the flowfield along the freejet axis, which is plotted in Fig. 14. The freezing of the parallel temperature for argon at a higher value than that for helium is shown. The behavior is consistent with simple physical agreements as well as other analytical solutions. The perpendicular temperature, which is also plotted in Fig. 14, shows the continuation of the $T \sim r^{-4/3}$ inviscid temperature dependence. Qualitatively

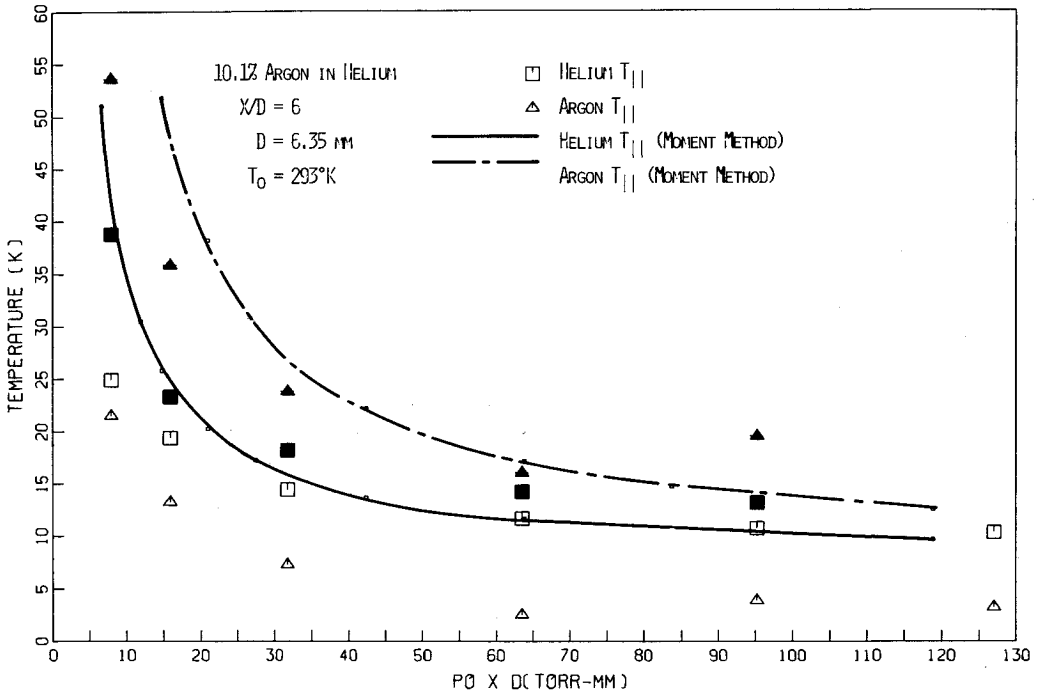

Fig. 13 Parallel temperature as a function of source pressure for 10.1% argon in helium (solid symbols are Monte Carlo calculations).

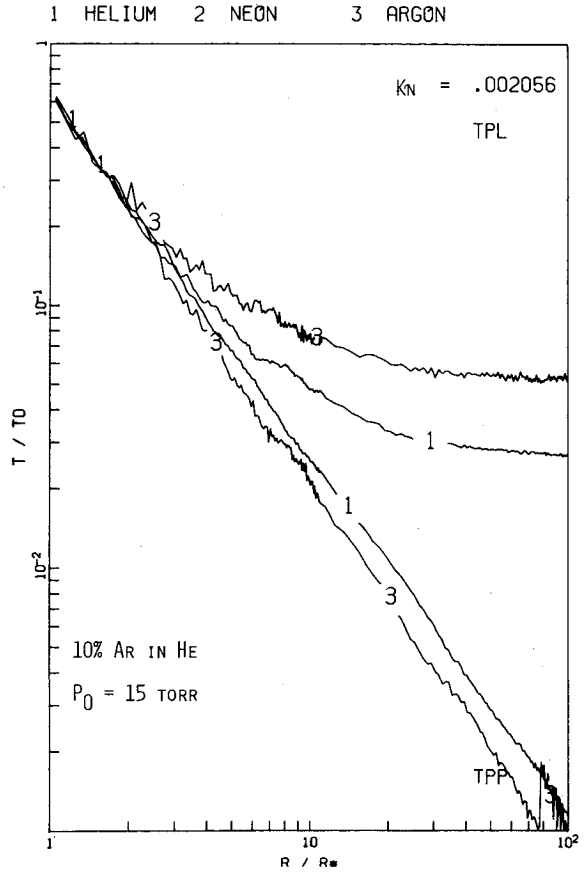

Fig. 14 Monte Carlo simulation of the parallel and perpendicular temperature distribution along the jet centerline for 10% argon in helium.

similar behavior between the measured parallel temperature, and moment solutions results are observed for both the 9.5% neon in helium (Fig. 15) and the ternary mixture (Fig. 16). For both analytical methods, the heavy molecular weight species freezes at a higher parallel temperature.

The experimental meaurements which show the lighter molecular weight species freezing out at a higher temperature than the light carrier gas is not consistent with previous molecular beam experiments. The heavier molecular weight species carry more internal energy because of their large mass and, therefore, require more collisions with the lighter carrier gas to approach thermal equilibrium. They would be expected to have their internal energy frozen at higher temperatures. Experimentally, this lower temperature could be the result of a line-broadening effect in the argon and neon spectral lines, which was present in the calibration measurements but not in the lower density, velocity slip experiments. At present, this anomalous behavior has not been explained and requires further study. Although the measured argon and neon temperatures have been used for further comparison with theory, this comparison should be annotated with awareness of the problem.

For the ternary gas mixtures, the velocity and temperature of the individual species can be used to construct velocity distribution functions from which a separation efficiency can be determined. In Fig. 17, the argon, neon, and helium velocity distributions based on a set of experimental measurements are presented. The distribution functions have been normalized by the peak of the helium distribution function. If a separation is made with a velocity cut at the midpoint of the differential slip velocity between argon and helium, a separation factor,[22] α can be defined:

$$\alpha = \frac{n_{\mathrm{Ar}_L} n_{\mathrm{Ne}_R}}{n_{\mathrm{Ar}_R} n_{\mathrm{Ne}_L}} \tag{6}$$

where n_{Ar_L} is the total number of argon molecules with velocity to the left of the cut and n_{Ar_R} is the total number of agron molecules with velocities to the right of the cut. Similar definitions follow for the two neon streams n_{Ne_R} and n_{Ne_L}. These quantities can be defined by:

$$n_{\mathrm{Ar}_L} = \frac{1}{2} n_{\mathrm{Ar}} \left\{ 1 + \mathrm{erf}\left[\frac{\Delta \tilde{u}}{2} \left(\frac{m_{\mathrm{Ar}}}{2kT_{\mathrm{Ar}}} \right)^{1/2} \right] \right\}$$

$$n_{\mathrm{Ar}_R} = \frac{1}{2} n_{\mathrm{Ar}} \left\{ 1 - \mathrm{erf}\left[\frac{\Delta \tilde{u}}{2} \left(\frac{m_{\mathrm{Ar}}}{2kT_{\mathrm{Ar}}} \right)^{1/2} \right] \right\}$$

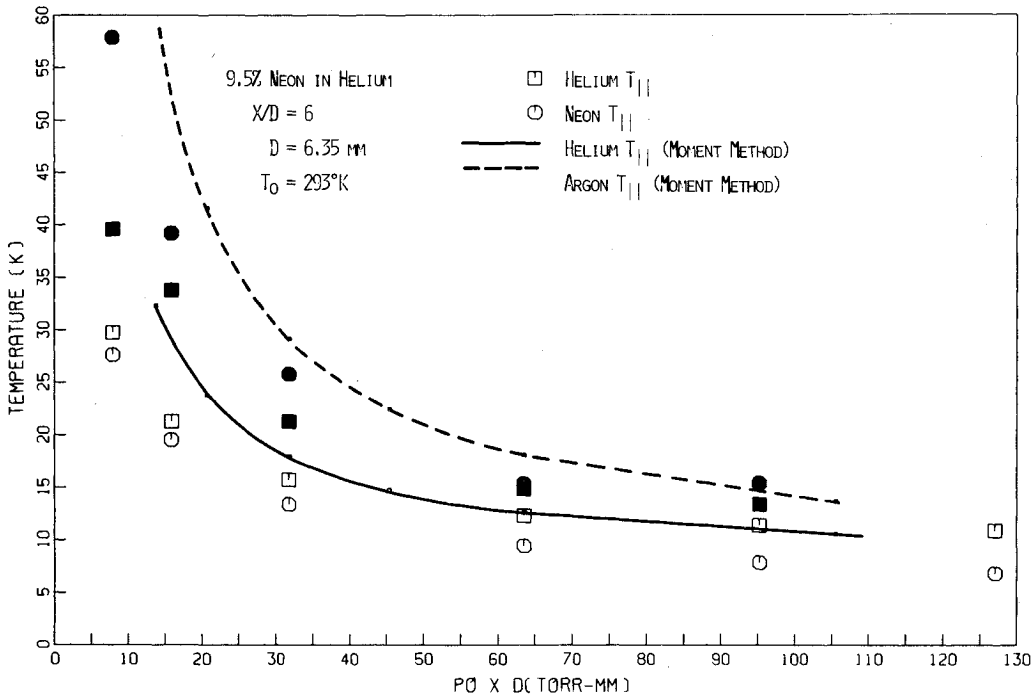

Fig. 15 Parallel temperature as a function of source pressure for 9.5% neon in helium (solid symbols are Monte Carlo calculations).

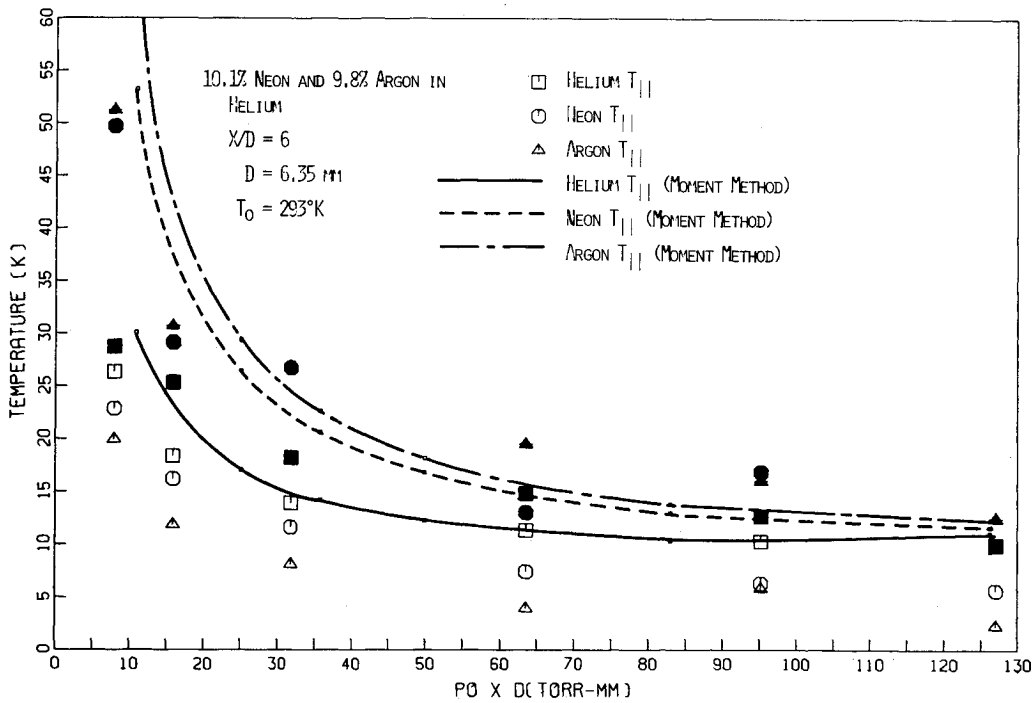

Fig. 16 Parallel temperature as a function of source pressure for 10.1% neon and 9.8% argon in helium (solid symbols are Monte Carlo calculations).

$$n_{\mathrm{Ne}_L} = \frac{1}{2} n_{\mathrm{Ne}} \left\{ 1 - \mathrm{erf}\left[\frac{\Delta \bar{u}}{2} \left(\frac{m_{\mathrm{Ne}}}{2kT_{\mathrm{Ne}}} \right)^{1/2} \right] \right\}$$

$$n_{\mathrm{Ne}_R} = \frac{1}{2} n_{\mathrm{Ne}} \left\{ 1 + \mathrm{erf}\left[\frac{\Delta \bar{u}}{2} \left(\frac{m_{\mathrm{Ne}}}{2kT_{\mathrm{Ne}}} \right)^{1/2} \right] \right\} \quad (7)$$

where $\bar{u}$ is the differential velocity slip between argon and neon. The vertical line through the argon and neon distribution functions in Fig. 17 shows the position of the velocity cut. With these definitions, a separation factor $\alpha = 2.13$ can be calculated for this case.

Separation factors for argon in the ternary mixture in the experiment are, in general, always higher than the Monte Carlo simulation and moment methods results. This is due primarily to the lower argon and neon temperatures obtained in the experiments, the differential velocity slip being in good agreement and not contributing significantly to the difference. Because of the lower trace species temperatures and uncertainty in their accuracy, it is not clear that the peak observed in the experimental separation factor is a real effect. Background gas penetration of the freejet could thermalize the gas and explain a peaking in the separation factor. A systematic study of the effect of background gas pressure on the jet gas temperature at the measurement position would be required to support such an explanation.

The point to be made in this comparison between experiment and theory is the importance of the translational nonequilibrium and the resulting parallel temperature in predicting the separation factor. Both analytical and ex-

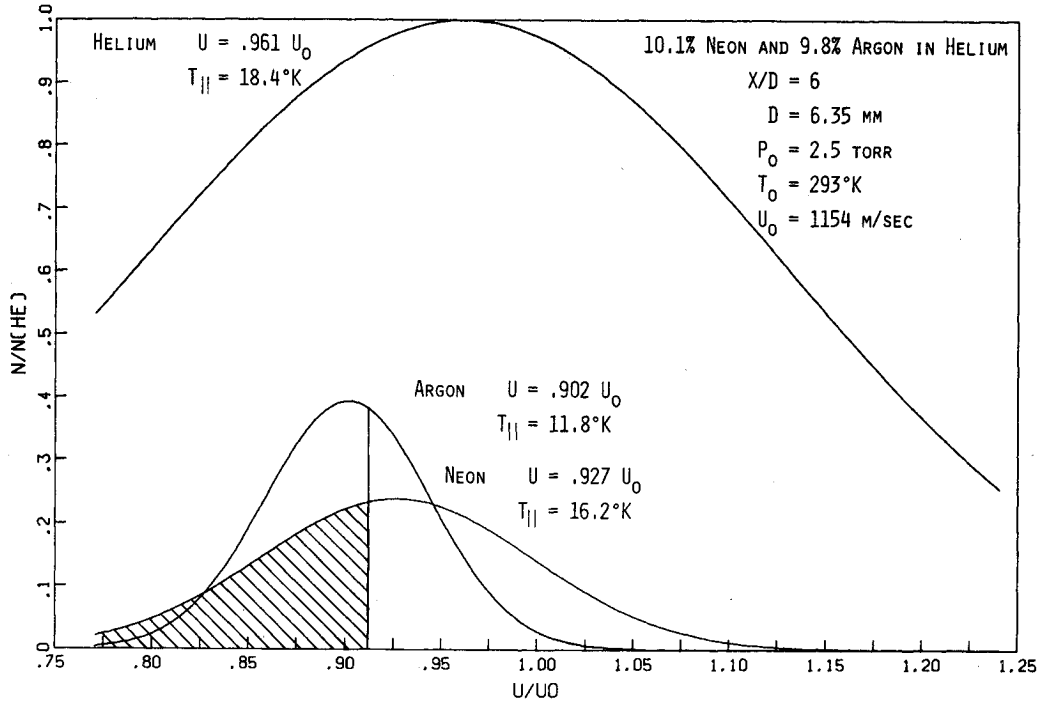

Fig. 17 Helium, argon, and neon velocity distribution functions from measured temperatures and velocities.

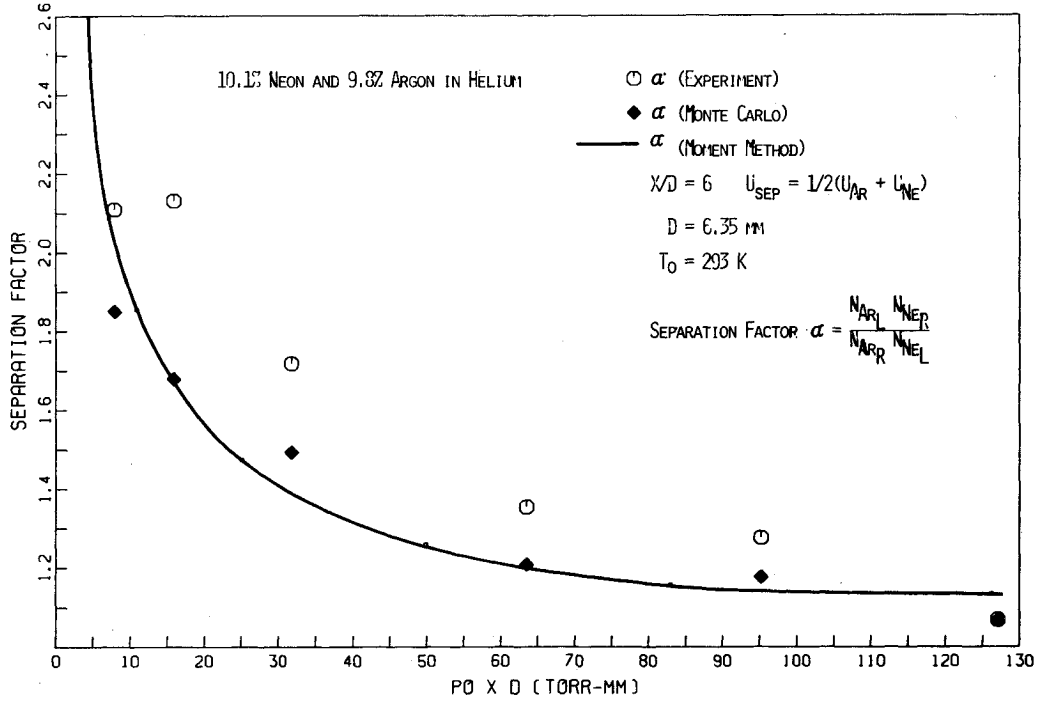

Fig. 18 Argon separation factor for 10.1% neon and 9.8% argon in helium as a function of source pressure.

perimental separation factors would be expected to improve somewhat with any decrease in the parallel temperature or increase in the differential velocity slip further downstream from the position that was studied. From the moment method calculations,[7] an increase of at most 15% could be expected in the velocity slip further downstream in the jet. The parallel temperatures which are nearer their terminal values would be expected to decrease even less. As mentioned before, the temperatures would eventually increase due to the effect of background gas penetration.

It is interesting to compare the maximum separation factor $\alpha = 2.13$ found from the experimental results with the equivalent separation factor for a diffusive separation of argon and neon, which is based on their mass ratio, $\alpha_d = (m_{Ar}/m_{He})^{1/2} = 1.4$. The factor α, as previously defined, is a measure of the degree of separation given by the process. Although the velocity slip based on the experiments yields a 50% larger separation factor than diffusion, its advantage could be even greater when viewed in economic terms. To compare the economics of different separation processes, a useful measure is the separative work factor δw[22] per stage.

$$\delta w = L(1-\theta)(\alpha - 1)^2 \tag{8}$$

where L is the molar throughput of separated isotopes, θ is the fraction of separated isotopes leaving in one exit stream, and $1-\theta$ is the fraction leaving in the other exit stream. Assuming equal molar throughput and the same fraction of separated isotopes θ, the important factor to be compared is $(\alpha-1)^2$. Using this as a basis, the velocity slip process would require a

factor of eight fewer stages than a diffusion process to produce the same amount of separative work for separating argon and helium. It should be noted that this conclusion is based on a somewhat speculative assumption of equal molar throughout.

Summary and Conclusions

Both velocity slip and translational temperatures were observed along the axis of an axisymmetric freejet expansion for both binary and ternary mixtures of argon and neon in helium. A Monte Carlo simulation of the experiment indicates that the velocity slip can be modeled with reasonable accuracy—on the order of a few percent. The parallel translational temperatures for the heavy molecular weight species, which are critical to an isotope separation process, were measured and found to be lower when compared to either the Monte Carlo simulation or moment method analysis. This result leads to measured separation efficiencies somewhat higher than predicted. A maximum separation factor $\alpha = 2.13$ for argon was calculated from the measured temperatures and differential velocity slip for a mixture of argon and neon in helium. When this result is compared to the equivalent diffusive separation factor $\alpha = 1.4$ for argon and neon, the improvement in separative work done per separation stage could be as high as eight times greater using velocity slip. Neither of these processes are practical schemes for an argon-neon separation when compared to a direct distillation process. The point to be stressed, however, is the relative effectiveness of the velocity slip technique when compared with diffusion. Certainly, other economic factors would have to be included in any comparison of such separation schemes for gases of practical interest. Nevertheless, the advantage in separation factor, demonstrated both experimentally and analytically with this argon-neon example does provide support for the previous work with regard to separating $^{235}UF_6$ and $^{238}UF_6$.

Acknowledgment

This work could not have been done without the cooperation of the University of California, Dept. of Mechanical Engineering, Berkeley. The support of this work by Sandia Laboratories is most appreciated. G. Miller's assistance in running the Monte Carlo simulation codes was invaluable. G. Lewis' skill in the setup of the experiments is also gratefully acknowledged.

References

[1] Touryan, K. J., Muntz, E. P., Talbot, L., and Von Halle, E., "Gas Dynamic Problems in Isotope Separation," SAND75-0121, NSF Workshop at Sandia Laboratories, Albuquerque, N. Mex., Dec. 1974.

[2] Anderson, J. B. and Davidovits, P., "Isotope Separation in a 'Seeded Beam'," *Science*, Vol. 187, Feb. 1975, pp. 642-644.

[3] Abuaf, N., Anderson, J. B., Andres, R. P., Fenn, J. B., and Marsden, P.G.H., "Molecular Beams with Energies above One Electron Volt," *Science*, Vol. 155, Feb. 1967, pp. 997-999.

[4] Miller, D. R. and Andres, R. P., "Translational Relaxation in Low Density Supersonic Jets," *Proceedings of the Sixth International Sympsoium on Rarefied Gas Dynamics*, Vol. II, edited by L. Trilling and H. V. Wachman, Academic Press, New York, 1969, pp. 1385-1402.

[5] Patch, D. F., "Application of Free Jet Sources to Reactive Crossed Molecular Beam Experiments," Ph.D. Dissertation, University of California, San Diego, Calif., 1977.

[6] Haberland, H., Tully, F. P., and Lee, Y. T., "Hyperthermal Xe Beam from Free Jets of 1% Xe and 99% H_2," *Book of Abstracts, Eighth International Symposium on Rarefied Gas Dynamics*, Vol. II, edited by K. Karamcheti, Academic Press, New York, 1974, pp. 533-538.

[7] Cattolica, R. J., Gallagher, R. J., Talbot, L., Willis, D. R., Hurlbut, F. C., Fizdon, W., and Anderson, J. B., "Research on Aerodynamic Means of Isotope Separation," Sandia Laboratories Energy Rept. SAND78-8216, Livermore, Calif., March 1978.

[8] Muntz, E. P., "The Electron Beam Fluorescence Technique," NATO AGARDograph 132, Dec. 1968.

[9] Jacquinot, P., "New Developments in Interference Spectroscopy," *Progress in Physics*, Vol. 23, p. 267.

[10] Ashkenas, H. and Sherman, F. S., "The Structure and Utilization of Free Jet Expansion," *Rarefied Gas Dynamics*, J. H. de Leeum (Ed.), Academic Press, New York, 1966.

[11] Cattolica, R. J., Robben, F., Talbot, L., and Willis, D. R., "Translational Nonequilibrium in Free Jet Expansions," *The Physics of Fluids*, Vol. 17, Oct. 1974, pp. 1743-1807.

[12] Brook, J. W. and Oman, R. A., "Steady Expansion of High-Speed Ratio Using the BKG Kinetic Model," *4th Symposium on Rarefied Gas Dynamics*, Vol. I, 1964, p. 125.

[13] Hamel, B. B. and Willis, D. R., "Kinetic Theory of Source Expansion with Application to the Free Jet," *The Physics of Fluids*, Vol. 9, 1966, p. 829.

[14] Cooper, A. L. and Bienkowski, G. K., "An Asymptotic Theory for Steady Source Expansion of a Binary Mixture," *5th Symposium on Rarefied Gas Dynamics*, Vol. I, 1966, p. 861.

[15] Anderson, J. B., "Intermediate Energy Molecular Beams from Free Jets of Mixed Gases," *Entropie*, Vol. 18, 1967, p. 33.

[16] Bird, G. A., *Molecular Gas Dynamics*, Oxford University Press, Oxford, England, 1976.

[17] Bird, G. A., "Breakdown of Translational and Rotational Equilibrium in Gaseous Expansions," *AIAA Journal*, Vol. 8, 1970, p. 1998.

[18] Raghuraman, P., Davidovits, P., and Anderson, J. B., "Isotope Separation by the Velocity Slip Process," edited by J. Leith Potter, Vol. 51, Pt. 1, *Progress in Aeronautics and Astronautics, Rarefied Gas Dynamics*, AIAA, New York, 1977.

[19] Hirschfelder, J. O., Curtis, C. F., and Bird, R. B., *Molecular Theory of Gases and Liquids*, John Wiley & Sons, Inc., New York, 1964.

[20] Cattolica, R. J., Gallagher, R. J., Anderson, J. B., and Talbot, L., "Velocity Slip and Translational Nonequilibrium of Ternary Gas Mixtures in Free Jet Expansions," AIAA Paper 77-704, Albuquerque, N. Mex., June 1977.

[21] Cattolica, R. J., Robben, F., and Talbot, L., "The Ellipsoidal Velocity Distribution Function and Translational Nonequilibrium," *Rarefied Gas Dynamics*, edited by M. Becker and M. Fiebig, DFVLR Press, Porz-Wahn, Germany, 1974.

[22] Dalgarno, A., Morrison, I. M., and Pengelly, R. M., "Long-Range Interactions between Atoms and Molecules," *International Journal of Quantum Chemistry*, Vol. 1, March 1967, pp. 161-167.

[23] Cohen, K., *The Theory of Isotope Separation as Applied to Large-Scale Production of ^{235}U*, McGraw-Hill, Book Co., Inc., New York, 1951.